

Accepted Manuscript

Title: Crystal Structure and Microwave Dielectric Properties of $\text{NaPb}_2\text{B}_2\text{V}_3\text{O}_{12}$ (B=Mg, Zn) Ceramics

Authors: Rakhi M., Subodh G.

PII: S0955-2219(18)30452-7
DOI: <https://doi.org/10.1016/j.jeurceramsoc.2018.07.023>
Reference: JECS 11991

To appear in: *Journal of the European Ceramic Society*

Received date: 1-4-2018
Revised date: 29-6-2018
Accepted date: 15-7-2018

Please cite this article as: Rakhi M, Subodh G, Crystal Structure and Microwave Dielectric Properties of $\text{NaPb}_2\text{B}_2\text{V}_3\text{O}_{12}$ (B=Mg, Zn) Ceramics, *Journal of the European Ceramic Society* (2018), <https://doi.org/10.1016/j.jeurceramsoc.2018.07.023>

This is a PDF file of an unedited manuscript that has been accepted for publication. As a service to our customers we are providing this early version of the manuscript. The manuscript will undergo copyediting, typesetting, and review of the resulting proof before it is published in its final form. Please note that during the production process errors may be discovered which could affect the content, and all legal disclaimers that apply to the journal pertain.



Crystal Structure and Microwave Dielectric Properties of NaPb₂B₂V₃O₁₂(B=Mg, Zn) Ceramics

Rakhi M. and Subodh G.*

Department of Physics
University of Kerala
Thiruvananthapuram-695581
Kerala, India.
*gsubodh@gmail.com

Abstract

Two low temperature sintered NaPb₂B₂V₃O₁₂ (B=Mg, Zn) ceramics with garnet structure were synthesized through conventional solid state reaction route and their crystal structure and microwave dielectric properties were investigated for the first time. Rietveld refinements of XRD patterns show both the compounds belong to cubic symmetry with space group *Ia-3d*. Observed number of Raman bands and group theoretical predictions also confirm cubic symmetry with space group *Ia-3d* for both NPMVO and NPZVO. At the optimum sintering temperature of 725°C NPMVO has a relative permittivity of 20.6 ± 0.2 , unloaded quality factor (Q_{uxf}) of $22,800 \pm 1500$ GHz ($f = 7.7$ GHz) and temperature coefficient of resonant frequency $+25.1 \pm 1$ ppm/°C while NPZVO has relative permittivity of 22.4 ± 0.2 , Q_{uxf} of $7,900 \pm 1500$ GHz ($f = 7.4$ GHz) and near zero temperature coefficient of resonant frequency of -6 ± 1 ppm/°C at 650°C. The relative permittivity of the compounds is inversely related to the corresponding Raman shifts.

Keywords: Crystal Structure, Raman Spectra, Garnet, Microwave Dielectric Properties

1. INTRODUCTION

Nowadays modern communication systems demand dielectric ceramics with temperature stability and stringent dielectric properties. The compactness, thermal stability, low cost of production, high efficiency, and adaptability to microwave integrated circuits (MICs) are the main advantages of ceramic materials over other materials. These ceramics have the main application in the field of mobile communication, satellite navigation, guiding and positioning system and radar and global positioning system. These materials are widely used as dielectric resonators, duplexer, dielectric waveguide and microwave substrates etc. Ceramics with large $Q \times f$, nearly zero τ_f and ϵ_r ranging from 20 to 100 are used for wide range of applications from 800 MHz to 20 GHz of the microwave spectrum, which includes base station resonators/antenna Substrate application, which need relative permittivity in the range of 20 to 50, higher bandwidth antenna substrates applications where $5 < \epsilon_r < 20$ and $60 < \epsilon_r < 70$ for base station resonators applications. Besides this these types of materials have immense applications in the field of Low temperature co-fired ceramic technology, when they are chemically compatible with inner electrodes such as Al/Ag.

For dielectric resonator applications, ceramics should possess high unloaded quality factor ($Q_u \times f$) which means low dielectric loss for selectivity, high dielectric constant (ϵ_r) for miniaturization and zero temperature coefficient of resonant frequency (τ_f) for temperature stability [1-7].

Literature review provides numerous dielectric material with suitable relative permittivity and high $Q \times f$ values [8] for various applications, which includes Li_2O rich compounds, TeO_2 containing compounds and Bi_2O_3 rich compounds etc [9-16]. Sebastian *et al.* and Sreemoolanadhan *et al.* reported several dielectric resonators having Ti and Ba content [17-20].

Because of appropriate relative permittivity, high-quality factor, and low-sintering temperature, vanadate compounds were thought to be the promising candidate for microwave applications. Wang *et al.* reported BVO_4 ($\text{B} = \text{La}, \text{Ce}$) ceramics sintered at 850 and 750°C possess dielectric properties: $\epsilon_r = 14.2$ and 12.3, $Q_{\text{u}}\text{xf} = 48,197$ and 41,460 GHz, and $\tau_f = -37.9$ and -34.4 ppm/°C [21]. Suresh *et al.* reported some vanadate based compounds which possess very high quality factors. Among them, $\text{Ba}_3\text{TiV}_4\text{O}_{15}$ ceramic sintered at the optimum sintering temperature of 800°C possess a Relative permittivity of 13.6, unloaded quality factor of 31,800 and $\tau_f = 10$ ppm/°C and $\text{Ba}_3\text{ZrV}_4\text{O}_{15}$ sintered at 800°C possess a Relative permittivity of 10.7, $Q_{\text{u}}\text{xf} = 30600$ and $\tau_f = -102$ ppm/°C [22]. Umemura *et al.* reported that $\text{Mg}_3(\text{VO}_4)_4$ ceramics sintered at 950°C/50h possess a Relative permittivity of 9.1, $Q_{\text{u}}\text{xf} = 64,142$ GHz and $\tau_f = -93.2$ ppm/°C [23]. Li *et al.* reported that $\text{Ca}_5\text{Co}_4\text{V}_{5.95}\text{O}_{24-0.1}\text{TiO}_2$ ceramics is having a dielectric constant of 13.7, $Q_{\text{u}}\text{xf} = 19,159$ GHz and $\tau_f = 0$ ppm/°C [24]. $\text{Ca}_5\text{Mn}_4(\text{VO}_4)_6$ ceramics sintered at 875°C showed dielectric properties: $\epsilon_r = 11.2$, $Q_{\text{u}}\text{xf} = 33,800$ GHz, and $\tau_f = -70$ ppm/°C [25].

Compounds with the nominal composition $\text{A}_3\text{B}_2\text{C}_3\text{O}_{12}$ are known as garnets. In the garnet structure, three different sites (A, B, and C) are available for a wide variety of cations substitution, where C ions are surrounded by four oxygen to form CO_4 tetrahedron, B ions are located in octahedra. The tetrahedra and octahedra are corner shared, forming dodecahedra where the A ions are located [26]. Zhou *et al.* [27] reported that $\text{Na}_2\text{BiMg}_2\text{V}_3\text{O}_{12}$ ceramics sintered at 660°C/4h exhibit excellent microwave dielectric properties such as $\epsilon_r = 23.2$, $Q_{\text{u}}\text{xf} = 3700$ GHz and $\tau_f = 8.2$ ppm/°C. Fang *et al.* [28] reported that $\text{NaCa}_2\text{Mg}_2\text{V}_3\text{O}_{12}$ sintered at 915°C/4h exhibit dielectric constant of 10, $Q_{\text{u}}\text{xf} = 50600$ and $\tau_f = -47$ ppm/°C. Yao *et al.* [29] studied $\text{Ca}_5\text{Mg}_4(\text{VO}_4)_6$ sintered at 800°C possess relative permittivity of 9.2, $Q_{\text{u}}\text{xf} = 53,300$ and $\tau_f = -80$ ppm/°C. In 1975 Neurgaonkar and Hummel reported a series of novel garnet compounds

including $\text{NaPb}_2\text{B}_2\text{V}_3\text{O}_{12}$ (B=Mg, Zn) [30]. In search for another microwave dielectric material with low sintering temperature we synthesized $\text{NaPb}_2\text{B}_2\text{V}_3\text{O}_{12}$ (B=Mg, Zn) ceramics and its crystal structure as well as dielectric properties are investigated for the first time.

2. EXPERIMENTAL METHODS

The compounds $\text{NaPb}_2\text{B}_2\text{V}_3\text{O}_{12}$ (B=Mg, Zn) were prepared through conventional solid state reaction route using high purity Na_2CO_3 (Alfa aesar, 99.5%) ZnO , MgO , PbO and NH_4VO_3 (Sigma Aldrich, >99%). The compounds were ball milled using ceria stabilized zirconia balls in acetone medium for 24 hours. NMPVO and NZPVO were calcined at 650 and 600°C respectively. The phase purity and crystal structure of the calcined samples were studied by X-Ray Diffraction technique using $\text{Cu } K\alpha$ radiation ($\lambda = 1.5406 \text{ \AA}$) in a BrukerD8 Advance Diffractometer in the 2θ range of 5-120°. TOPAS 4.2 software was used for the Rietveld refinement. Renishaw Laser Raman Micro spectrometer with excitation wavelength of 785 (300 mW), in the spectral range from 100 to 4000 cm^{-1} and having spectral resolution is 1 cm^{-1} was used for recording Raman spectra. For dielectric measurements the calcined powders were ground and mixed with PVA solution. The slurries were dried and pressed into cylindrical pellets having diameter 10 mm and 1-2 mm thickness for radio frequency measurements and diameter of 10 mm and thickness of 5 mm for microwave measurements. Densities of the samples were measured using Archimedes method. The green pellets were sintered at the optimum sintering temperature of 725 and 650°C respectively for NPMVO and NPZVO. The surface morphology of the samples was analyzed using a scanning electron microscope (ZEISS EVO 18). Sintered and polished pellets were etched below 25°C of their respective sintering temperatures and used for the microstructural analysis. The radio frequency dielectric properties were studied using a LCR meter (HIOKI 6582). Microwave dielectric properties were measured

using a Network analyzer (ROHDE & SCHWARZ, ZV-Z135). The dielectric constant and unloaded quality factor of the samples were measured using TE_{01δ} mode cavity. The temperature coefficient of resonant frequency τ_f was measured by noting the variations of TE_{01δ} mode frequency with temperature in the range of 25-85°C. The temperature coefficient of the resonant frequency τ_f values were calculated using the formula as follows:

$$\tau_f = \frac{f_{85} - f_{25}}{60 * f_{25}} * 10^6 \text{ ppm/}^\circ\text{C} \quad (1)$$

where, f_{85} and f_{25} are the resonant frequencies at the measuring temperatures 85 and 25 °C, respectively.

3. RESULTS AND DISCUSSION

The room temperature XRD patterns of NPMVO and NPZVO ceramics calcined at 650 and 600°C are shown in Fig.S1. The crystalline nature of the compounds is clearly evident from the sharper diffraction peaks at respective diffraction angles, which can be indexed based on space group *Ia-3d* (ICDD File No. 00-024-1104). In order to study the crystal structure in detail Rietveld refinement of the XRD patterns were done using TOPAS 4.2 software, and are shown in Figs. 1-2. The obtained refinement parameters are $R_p = 3.56\%$, $R_{wp} = 4.84\%$ and $\chi^2 = 1.90$ for NPMVO, $R_p = 3.14\%$, $R_{wp} = 4.25\%$ and $\chi^2 = 1.61$ for NPZVO. Table 1-2 shows the refined crystallographic parameters for both the compounds. The refined lattice parameters obtained are $a = 12.7499(3) \text{ \AA}$ and $a = 12.7578(1) \text{ \AA}$ for NPMVO and NPZVO respectively. The crystal structure of these compounds belongs to the space group *Ia-3d* in which each unit cell contains eight molecules. The cations in the A site, B and C site have 8, 6 and 4 nearest oxygen neighbours and they are located in *24c*, *16a* and *24d* Wyckoff sites, the oxygen anions occupied in

the $96h$ site depend on the space coordinate. The inset of Figs.1-2 shows the polyhedral representation of crystal structure of NPMVO and NPZVO. It can be noted that Na^+ and Pb^{2+} are randomly occupied 8 coordinated A site, while Mg^{2+} , Zn^{2+} are occupied in 6 coordinated B site and V^{5+} is occupied 4 coordinated C site.

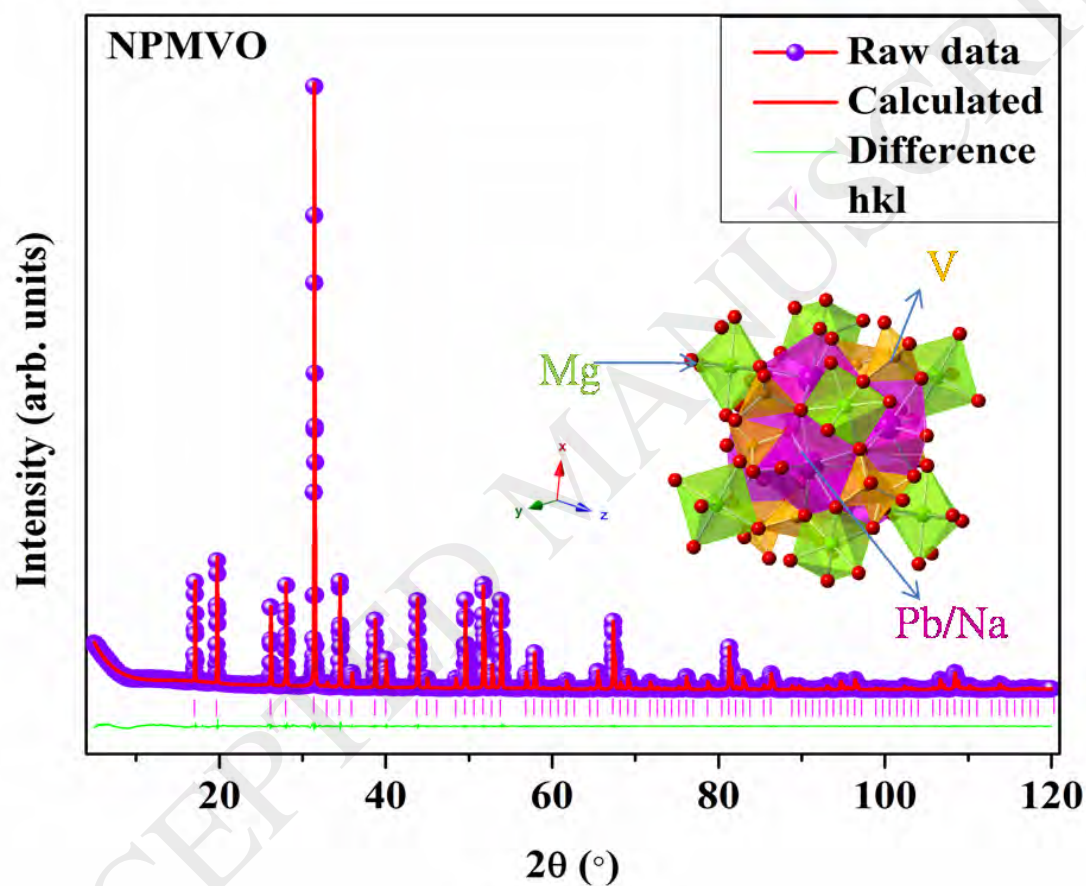


Fig.1. Rietveld refinement of X-Ray diffraction pattern of NPMVO ceramics calcined at 650°C.

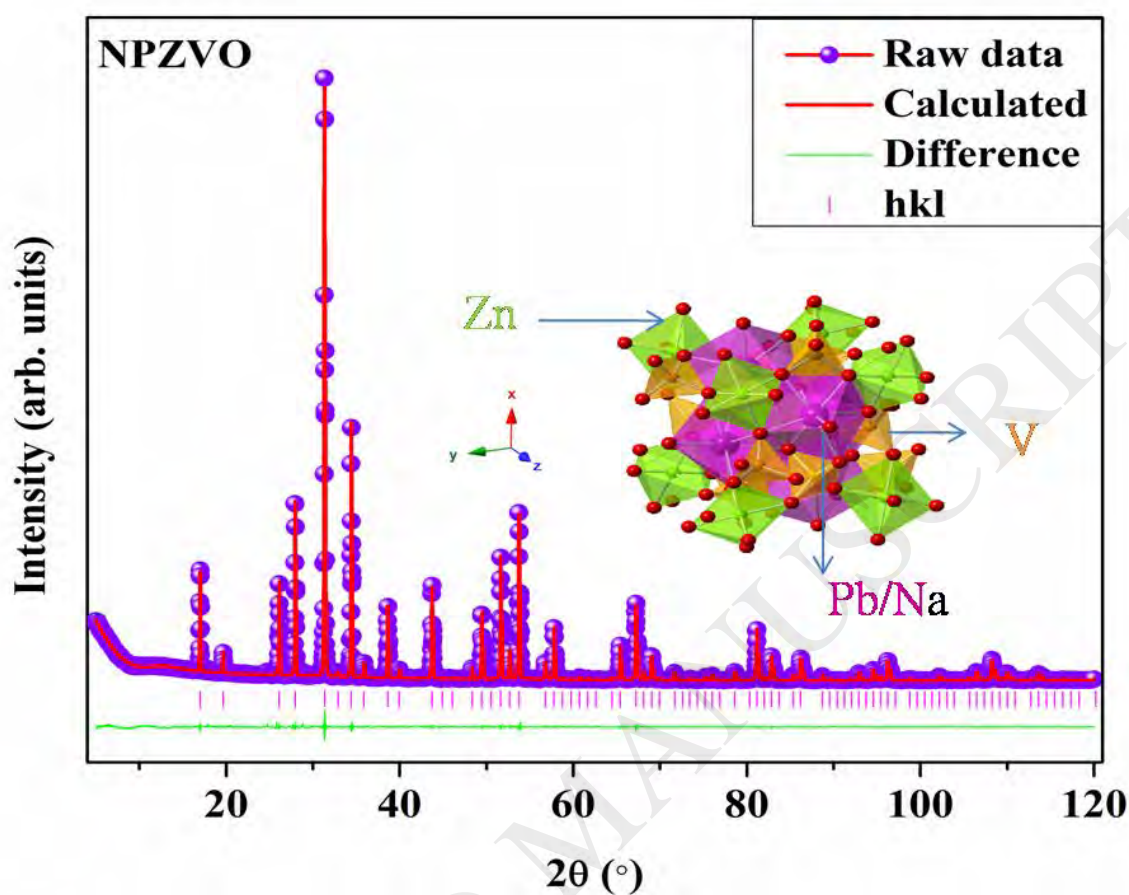


Fig.2. Rietveld refinement of X-Ray diffraction pattern of NPZVO ceramics calcined at 600°C.

Table 1. Refined crystallographic parameters for NPMVO ceramics.

| Atom | Site | x | y | z | Occupancy | B_{eq} (\AA^2) |
|------|------|---------|---------|---------|-----------|--------------------------------|
| Pb1 | 24c | 0.37500 | 0.50000 | 0.25000 | 0.6667 | 1.026 |
| Na1 | 24c | 0.37500 | 0.50000 | 0.25000 | 0.3333 | 0.7525 |

| | | | | | | |
|------------|------------|---------|---------|---------|---|--------|
| Mg1 | <i>16a</i> | 0.50000 | 0.50000 | 0.00000 | 1 | 0.6411 |
| V1 | <i>24d</i> | 0.62500 | 0.50000 | 0.25000 | 1 | 0.4627 |
| O1 | <i>96h</i> | 0.54050 | 0.55138 | 0.15517 | 1 | 0.758 |

Table 2. Refined crystallographic parameters for NPZVO ceramics.

| Atom | Site | <i>x</i> | <i>y</i> | <i>z</i> | Occupancy | B_{eq} (Å²) |
|-------------|-------------|-----------------|-----------------|-----------------|------------------|---|
| Pb1 | <i>24c</i> | 0.37500 | 0.50000 | 0.25000 | 0.6445 | 1.148 |
| Na1 | <i>24c</i> | 0.37500 | 0.50000 | 0.25000 | 0.3333 | 0.7525 |
| Zn1 | <i>16a</i> | 0.50000 | 0.50000 | 0.00000 | 1 | 0.6411 |
| V1 | <i>24d</i> | 0.62500 | 0.50000 | 0.25000 | 1 | 0.91 |
| O1 | <i>96h</i> | 0.54286 | 0.54423 | 0.15517 | 1 | 0.758 |

Fig. S2 shows the room temperature Raman spectrum of the compounds from 100 to 1000 cm^{-1} and Fig. 3 shows the deconvoluted Raman spectra of NPMVO and NPZVO. The factor group analysis predicts that for garnet structure there exist 98 vibration modes at the Brillouin zone center as given in equation 2, in which 55 of them are silent and one of them has acoustic in nature [31-33]. The remaining are IR and Raman active.

$$3A_{1g} + 5A_{2g} + 8E_g + 14T_{1g} + 14T_{2g} + 5A_{1u} + 5A_{2u} + 10E_u + 18T_{1u} + 16T_{2u} \quad (2)$$

In which 17 IR active and 25 Raman active modes are present. The Raman active modes include $3A_{1g} + 8E_g + 14F_{2g}$, where A_{1g} , E_g and F_{2g} corresponding to internal modes, translational and rotatory modes respectively [34]. A_{1g} mode has the maximum intensity, which belongs to the stretching and bending vibration of VO_4 group. Further the high frequency bands above 600 cm^{-1} , which are linearly depending on lattice parameters, are related to the symmetric stretching of tetrahedral (VO_4) group. Fig. 3 shows 14 and 15 deconvoluted Raman active bands correspond to NPMVO and NPZVO respectively out of 25 predicted by factor group analysis. The detailed band assignments are provided in the Table S1. The presence of reduced number of Raman active bands found in these compounds may be due to the polycrystalline nature of samples, the overlapping of bands, low resolving power of instrument or the low intensity of bands. Raman shift and FWHM of Raman spectra for the internal stretching vibrational mode is shown in Table 3.

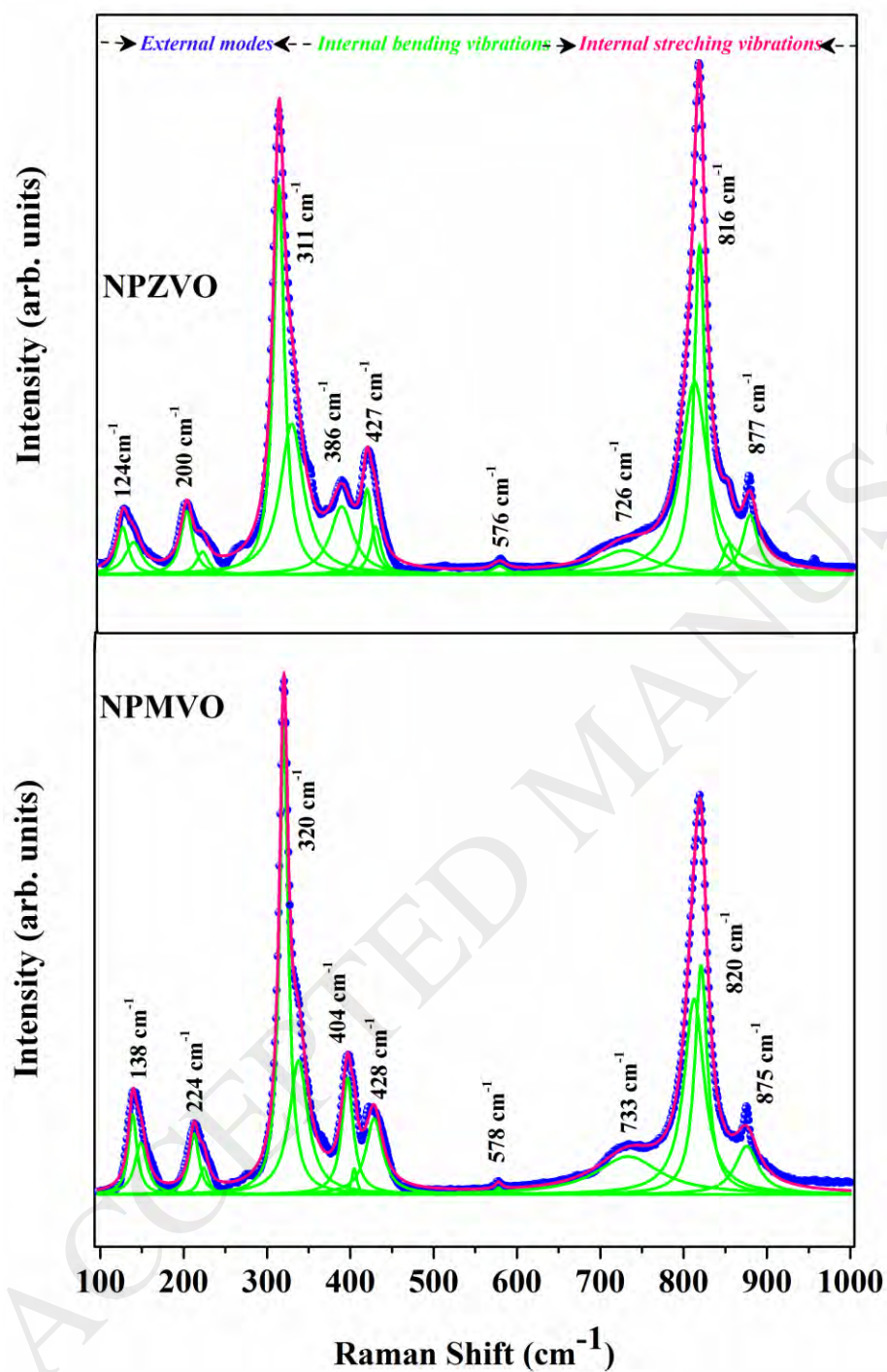


Fig.3. Deconvoluted Raman spectrum of NPMVO and NPZVO ceramics calcined at 650 and 600 $^{\circ}\text{C}$. Experimental data are in blue coloured solid circles while the fitting curve is in pink coloured line. Green line represents the phonon modes fitted using Lorentzian curve.

Fig. 4 represents the dependence of percentage density of NPMVO and NPZVO ceramics as a function of sintering temperature. For both NPMVO and NPZVO the relative density increases with increase in sintering temperature and then decreased with further increase in the temperature. The maximum density obtained for NPMVO is about of $93.6 \pm 0.1\%$ at 725°C and for NPZVO is about $92.3 \pm 0.1\%$ at 650°C respectively. When the sintering temperature increases beyond the optimum temperature both the compounds begin to melt and which in turn decrease the relative density. Fig. 5 (a) and (b) show the SEM micrographs of thermally etched NPMVO and NPZVO sintered at the optimum sintering temperature $725, 650^\circ\text{C}$ respectively. It shows a relatively dense microstructure with nearly uniform grain contrast. The grain size varies about 2 to $10\text{ }\mu\text{m}$ for NPMVO and an average of about $7\text{ }\mu\text{m}$ for NPZVO ceramics. It also worth to note that some of the grains are larger, which indicates grain growth has occurred confirming the low melting nature of these ceramics.

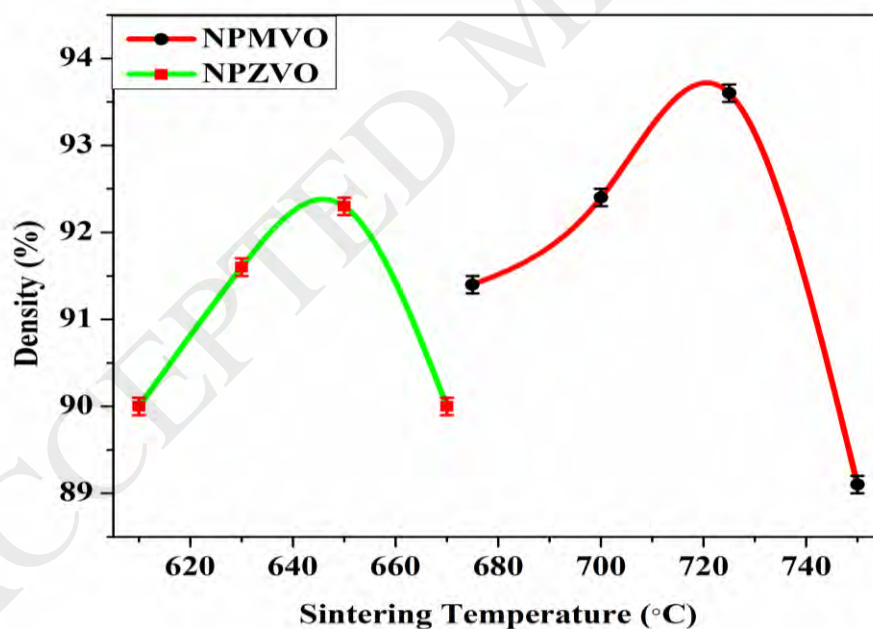


Fig. 4. Dependence of density on sintering temperature for NPMVO and NPZVO ceramics.

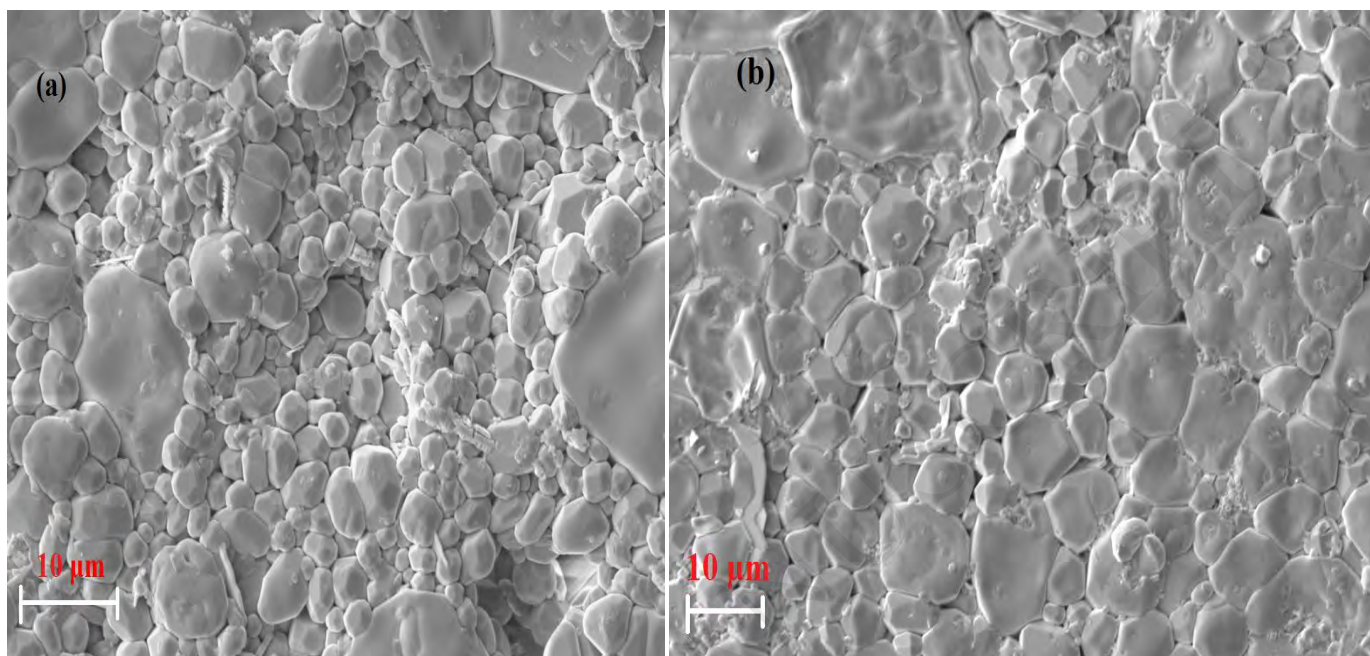


Fig. 5. (a) and (b) the microstructures of thermally etched NPMVO and NPZVO ceramics sintered at 725 and 650 °C respectively.

Figures S3-S4 shows the frequency dependence of Relative permittivity and dielectric loss of NMPVO and NPZVO at the optimum sintering temperature of 725 and 650°C respectively. At 1 MHz, the obtained Relative permittivity and dielectric loss of NPMVO, NPZVO were (24.5, 0.015) and (24.6, 0.037) respectively. As frequency increases the relative permittivity decreases and this can be attributed to the frequency dependent polarization mechanism (dipolar, atomic, ionic, and electronic) present in ceramics. As frequency increases the polarization ceases to exist one by one, which in-turn result in the drop of net polarization and hence decrease in dielectric constant. In the case of dielectric loss the material shows the similar trend of decrease in nature

as frequency increases. This can be due to the inability of the electron to follow the alternating frequency of AC electric field beyond certain critical frequency. Further, dielectric loss is mainly influenced not only by the lattice vibration modes but also by the porosity, micro cracks, densification, crystallite orientation, dislocations, secondary phases, grain boundaries and oxygen vacancies.

Microwave dielectric properties of NPMVO and NPZVO as the function of sintering temperature are shown in Figs. 6-7. As the sintering temperature increased the relative permittivity also increases up to its optimum sintering temperature and then decreases similar to the trend shown by density. The Relative permittivity of a material is mainly influenced by its relative density, dielectric polarisability and micro structural factors, which include grain boundaries, secondary phases, compositional homogeneity etc [29, 35-36]. In this case the variation in relative density is one of the reasons for the variation in relative permittivity with the change in sintering temperature. Even though NPMVO possesses better densification compared to NPZVO, it has a lower value of Relative permittivity. This may be due to the larger ionic polarisability of Zn^{2+} (2.04\AA^3) compared with Mg^{2+} (1.32\AA^3) [37]. Hence in this case the ionic polarisability is also one of the reasons for the difference in relative permittivity exhibited by these compounds. It was found that the relative permittivity showed an inverse correlation with Raman shift of vibration mode. In Fig. S2 the sharp and intense lines around 819 cm^{-1} for NPMVO, 815 cm^{-1} for NPZVO corresponds to the stretching modes of VO_4 groups respectively. When the larger Zn^{2+} ion replaced the smaller Mg^{2+} ion, the unit cell volume increases, which in turn affects the inter atomic distance in VO_4 tetrahedra and causing decrease in covalent bond between cation and VO_4 . This causes the shift of modes to the low frequency side. The similar result of inverse

relation between dielectric constant and Raman shift was reported by Wu et al. in compound $\text{Li}_2\text{Mg}_3\text{BO}_6$ (B=Ti, Sn, Zr) [38] and Zhang et al. in $\text{Ba}[\text{Mg}(1-x)/3\text{Zr}_x\text{Ta}_2(1-x)/3]\text{O}_3$ [39].

Figures 6 and 7 also show the dependence of $Q_{\text{u}}\text{xf}$ values as the temperature varies. In the case of NPMVO as the sintering temperature increases the $Q_{\text{u}}\text{xf}$ also increases to its maximum value for the optimum sintering temperature and then decreases, which is similar to the trend shown by density and relative permittivity. While in the case of NPZVO ceramics when the sintering temperature increases $Q_{\text{u}}\text{xf}$ shows a decreased value at the maximum densification. The microwave dielectric losses are mainly affected by many factors, which can be divided into two parts: one is the intrinsic loss and other is the extrinsic loss. The lattice vibration modes and crystal structure are mainly responsible for intrinsic losses in dielectrics. The main reason of dielectric loss is the anharmonic terms in the crystal potential energy. For the intrinsic loss, FWHM of the V-O stretching vibration given in Table S1 was taken into consideration. In general the lowest FWHM value has a highest quality factor. Eventhough NPZVO possesses low

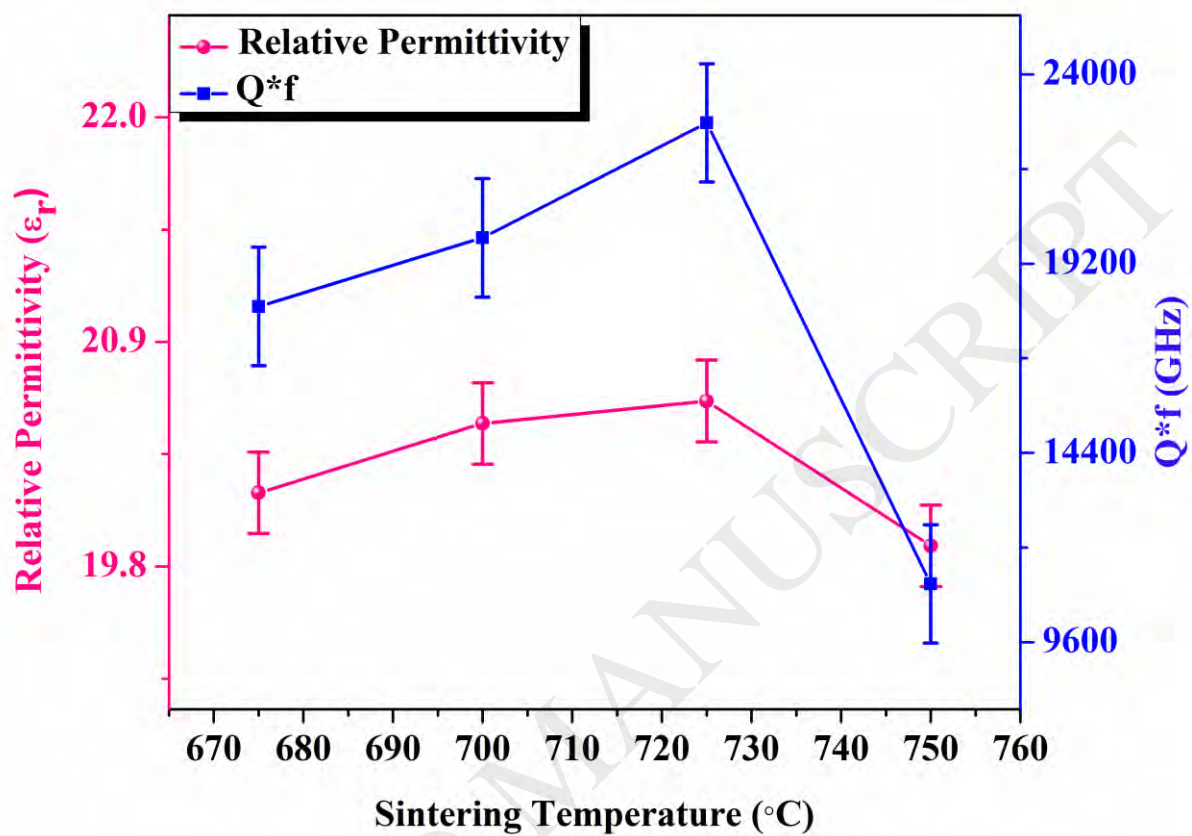


Fig.6. Dependence of Relative permittivity and $Q \cdot f$ on sintering temperature for NPMVO ceramics sintered at 725°C.

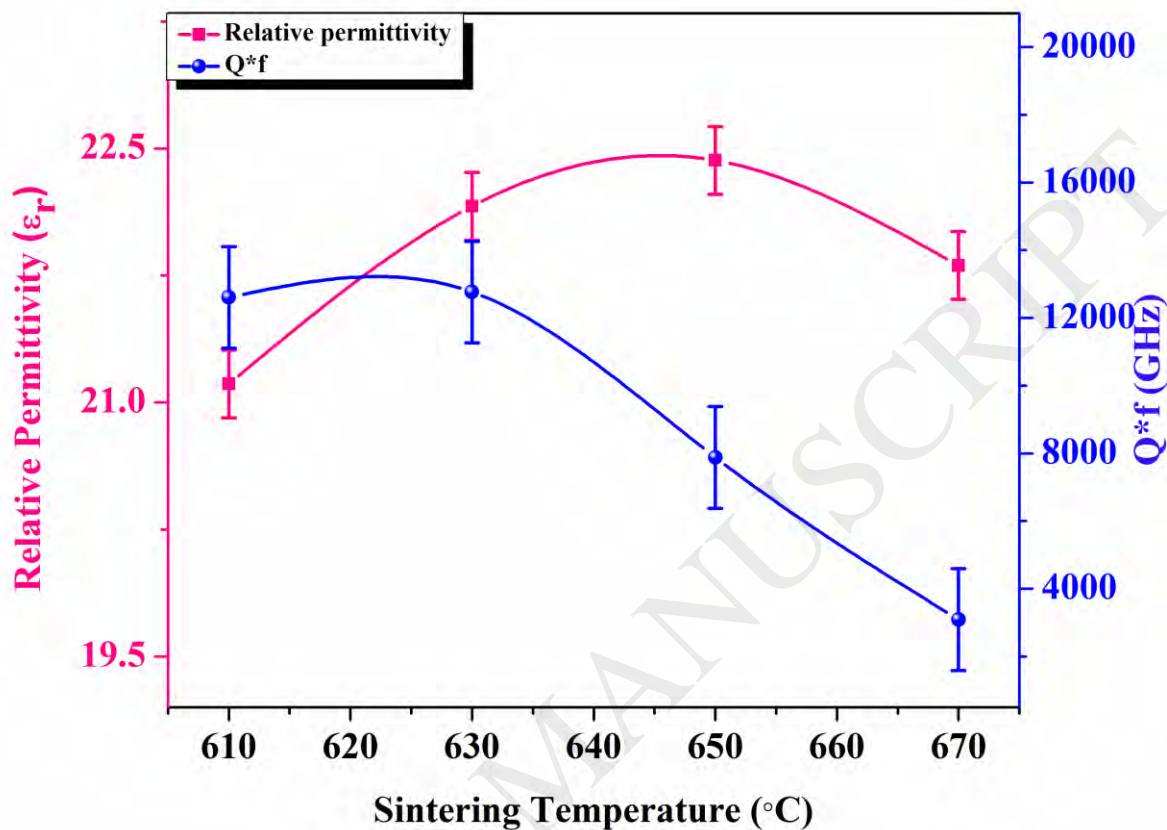


Fig.7. Dependence of Relative permittivity and Q_{uxf} on sintering temperature for NPZVO ceramics sintered at 650°C.

FWHM it show a lower value of Q_{uxf} compared with NPMVO. Hence in this case the extrinsic factors may be the primary reason for variation in quality factor. While extrinsic losses are influenced by so many factors, which includes secondary phases, impurity, cavity, substitution, oxygen vacancies, grain sizes and density [29,40-41]. In the present study Zn^{2+} has larger ionic polarisability compared to Mg^{2+} . So its larger ionic displacement polarization contributes to the overall microwave permittivity to NPZVO than NPMVO and cause the stronger oscillation in Zn^{2+} than Mg^{2+} at same structure and same atomic position and which inturn increase the losses and decrease in Q_{uxf} values in NPZVO ceramics. Further Fu *et al.* [42] reported that Q_{uxf} values

are closely related to packing fraction of the compound. Large the B site ion radius would increase the unit cell volume, which inturn decrease the packing fraction and obviously decrease the Q_{uxf} values. So the Q_{uxf} values are positively correlated to packing fraction in our case. A similar result was observed by Kim *et al.* in the case of ABO_4 ($A = Ca, Pb, Ba$; $B = Mo, W$) compounds [43]. At the optimum sintering temperature NPMVO ceramics exhibits relatively high Relative permittivity of 20.6 ± 0.2 and high unloaded quality factor (Q_{uxf}) around $22,800 \pm 1500$ GHz and a positive temperature coefficient of resonant frequency of 25.1 ± 1 ppm/ $^{\circ}C$ and NPZVO ceramics have Relative permittivity of 22.4 ± 0.2 , unloaded quality factor of $7,900 \pm 1500$ GHz and near zero temperature coefficient of resonant frequency of -6 ± 1 ppm/ $^{\circ}C$,

Table 3-Symmetric stretching modes and microwave dielectric properties

| Sample Name | Raman shift (cm^{-1}) | FWHM (cm^{-1}) | Relative permittivity (ϵ_r) | Q_{uxf} (GHz) | τ_f (ppm/ $^{\circ}C$) |
|-------------|---------------------------|--------------------|--|-------------------|------------------------------|
| NPMVO | 819 | 26.5 | 20.6 ± 0.2 | $22,800 \pm 1500$ | 25.1 ± 1 |
| NPZVO | 815 | 21 | 22.4 ± 0.2 | 7900 ± 1500 | -6 ± 1 |

4. Conclusions

Single-phase $NaPb_2B_2V_3O_{12}$ ($B=Mg, Zn$) ceramics were prepared through conventional solid-state ceramic route. XRD analysis and Raman spectra confirms that these ceramics have cubic garnet structure with space group $Ia-3d$. NPMVO ceramics has Relative permittivity of 20.6 ± 0.2 and high unloaded quality factor (Q_{uxf}) around $22,800 \pm 1500$ GHz and a positive temperature coefficient of resonant frequency of 25.1 ± 1 ppm/ $^{\circ}C$ at the optimized

sintering temperature. NPZVO ceramic has relatively higher Relative permittivity of 22.4 ± 0.2 , unloaded quality factor of $7,900 \pm 1500$ GHz and near zero temperature coefficient of resonant frequency of -6 ± 1 ppm/ $^{\circ}\text{C}$, which make them promising candidate for future microwave electronic applications.

Acknowledgement

Authors acknowledge the financial support received from Alexander von Humboldt foundation through equipment grant. Authors are thankful to SARD program of KSCSTE for the financial support.

References

- [1]H.Luo, W. Fang, L. Fang, W. Li, C. Li, Y. Tang, Microwave dielectric properties of novel glass-free low temperature firing $\text{ACa}_2\text{Mg}_2\text{V}_3\text{O}_{12}$ (A=Li, K) ceramics, *Ceram. Inter.*42 (2016) 10506–10510.
- [2]D.Zhou, H. Wang, X. Yao, L.-X. Pang, Sintering behavior, phase evolution, and microwave dielectric properties of $\text{Bi}(\text{Sb}_{1-x}\text{Ta}_x)\text{O}_4$ ceramics, *J. Am. Ceram. Soc.* 91 (2008) 2228–2231.
- [3]M.M.Krzman, M. Logar, B. Budic, D. Suvorov, Dielectric and microstructural study of the SrWO_4 , BaWO_4 , and CaWO_4 Scheelite ceramics, *J. Am. Ceram. Soc.* 94 (2011) 2464–2472.
- [4]L.Pang, D. Zhou, Z.-M. Qi, Z.-X. Yue, Influence of W substitution on crystal structure, phase evolution and microwave dielectric properties of $(\text{Na}_{0.5}\text{Bi}_{0.5})\text{MoO}_4$ ceramics with low sintering temperature, *Sci. Rep.* 7 (2017) 3201.
- [5]G. Subodh, R. Ratheesh, M.V. Jacob, M.T. Sebastian, Microwave dielectric properties and vibrational spectroscopic analysis of MgTe_2O_5 ceramics, *J. Mater. Res.* 23 (6) (2008) 1551-1556.

- [6] G. Subodh, M.T. Sebastian, Glass-Free $\text{Zn}_2\text{Te}_3\text{O}_8$ Microwave Ceramic for LTCC Applications, *J. Am. Ceram. Soc.* 90 (7) (2007) 2266–2268.
- [7] D. Zhou, L.-X. Pang, D. -W. Wang, C. Li, B. -B. Jin, I.M. Reaney, High permittivity and low loss microwavedielectrics suitable for 5G resonators and low temperature co-fired ceramic architecture, *J. Mater. Chem. C*, 5 (2017) 10094-10098.
- [8] L. Fang, C.X. Su, H.F. Zhou, Z.H. Wei, H. Zhang, Novel Low-Firing Microwave Dielectric Ceramic $\text{LiCa}_3\text{MgV}_3\text{O}_{12}$ with Low Dielectric Loss, *J. Am. Ceram. Soc.* 96 (3) (2013) 688–690.
- [9] H.F. Zhou, X.L. Chen, L. Fang, D.J. Chu, H. Wang, A New Low Loss Microwave Dielectric Ceramic for Low Temperature Co-fired Ceramic Applications, *J. Mater. Res.* 25 (2010) 1235–1238.
- [10] L. Fang, D.J. Chu, H.F. Zhou, X.L. Chen, Z. Yang, Microwave Dielectric Properties and Low Temperature Sintering Behavior of $\text{Li}_2\text{CoTi}_3\text{O}_8$ Ceramic, *J. Alloys Compd.* 509 (2011) 1880–1884.
- [11] S. George, M.T. Sebastian, Synthesis and Microwave Dielectric Properties of Novel Temperature Stable High Q, $\text{Li}_2\text{ATi}_3\text{O}_8$ (A=Mg, Zn) Ceramics, *J. Am. Ceram. Soc.* 93 (8) 2010 2164–2166.
- [12] D.-K. Kwon, M.T. Lanagan, T.R. Shrout, Microwave Dielectric Properties of $\text{BaO}-\text{TeO}_2$ Binary Compounds, *Mater. Lett.* 61 (2007) 1827–1831.
- [13] M. Udovic, M. Valant, D. Suvorov, Phase Formation and Dielectric Characterization of the $\text{Bi}_2\text{O}_3-\text{TeO}_2$ System Prepared in an Oxygen Atmosphere, *J. Am. Ceram. Soc.* 87 (4) (2004) 591–597.

- [14] M. Valant, D. Suvorov, Processing and Dielectric Properties of Sillenite Compounds $\text{Bi}_{12}\text{MO}_{20}$ ($\text{M}=\text{Si, Ge, Ti, Pb, Mn, B}_{1/2}\text{P}_{1/2}$), *J. Am. Ceram. Soc.* 84 (12)(2001)2900–2904.
- [15] D. Zhou, H. Wang, L.-X. Pang, C.A. Randall, X.Yao, Bi_2O_3 - MoO_3 Binary System: An Alternative Ultralow Sintering Temperature Microwave Dielectric, *J. Am. Ceram. Soc.* 92 (10) (2009) 2242–2246.
- [16] D. Zhou, C.A. Randall, H. Wang, L.-X. Pang, X. Yao, Microwave Dielectric Ceramics in Li_2O - Bi_2O_3 - MoO_3 System with Ultralow Sintering Temperature, *J. Am. Ceram. Soc.* 93 (4)(2010) 1096–1100.
- [17] M.T. Sebastian, S. Solomon, R. Ratheesh, Preparation, Characterization, and Microwave Properties of RETiNbO_6 ($\text{RE} = \text{Ce, Pr, Nd, Sm, Eu, Gd, Tb, Dy, Y, and Yb}$) Dielectric Ceramics, *J. Am. Ceram. Soc.* 87 (7)(2001) 1487-1489.
- [18] H. Sreemoolanadhan, M.T. Sebastian, P. Mohanan, Dielectric Ceramics in the $\text{BaO.Ln}_2\text{O}_3.5\text{TiO}_2$ Composition, *Ferroelectrics* 189 (1996) 43-46.
- [19] H. Sreemoolanadhan, M.T. Sebastian, P. Mohanan, High-Permittivity and Low-Loss Ceramics in the $\text{BaO-SrO-Nb}_2\text{O}_5$ System, *Mater. Res. Bull.* 16 (1995) 653–658.
- [20] S. Solomon, H. Sreemoolanadhan, M.T. Sebastian, P. Mohanan, Microwave Dielectric Resonators Based on $\text{Ba}((\text{Bi}_{0.2}\text{D}_{0.3})\text{Nb}_{0.5})\text{O}_3$ ($\text{D} = \text{Y, Pr, Sm, Gd, Dy, Er}$), *Mater. Lett.* 28(1996)107–111.
- [21] Y. Wang, R. Zuo, C. Zhang, J. Zhang, T. Zhang, Low - temperature - fired ReVO_4 ($\text{Re} = \text{La, Ce}$) microwave dielectric ceramics, *J. Am. Ceram. Soc.* 98(1) (2015) 1-4.
- [22] E.K. Suresh, A.N. Unnimaya, A. Surjith, R. Ratheesh, New vanadium based $\text{Ba}_3\text{MV}_4\text{O}_{15}$ ($\text{M}=\text{Ti and Zr}$) high Q ceramics for LTCC applications, *Ceram. Inter.* 39 (2013) 3635–3639.

- [23] R. Umemura, H. Ogawa, H. Ohsato, A. Kan, A. Yokoi, Microwave dielectric properties of low-temperature sintered $\text{Mg}_3(\text{VO}_4)_2$ ceramic, *J. Eur. Ceram. Soc.* 25 (2005) 2865–2870.
- [24] B. Li, J. Zheng, W. Li, Enhanced effect of vanadium ions non-stoichiometry on microwave dielectric properties of $\text{Ca}_5\text{Co}_4\text{V}_{6+x}\text{O}_{24}$ ceramics, *Mater. Chem. and Phys.* 207 (2018) 282–288.
- [25] G.-G. Yao, C.-J. Pei, P. Liu, J.-P. Zhou, H.-W. Zhang, Microwave dielectric properties of low temperature sintering $\text{Ca}_5\text{Mn}_4(\text{VO}_4)_6$ ceramics, *J. Mater. Sci. Mater. Electr.* 34 (2016) 2983–2987.
- [26] H.C. Xiang, L. Fang, X.W. Jiang, Y. Tang, C.C. Li, A Novel Temperature Stable Microwave Dielectric Ceramic with Garnet Structure: $\text{Sr}_2\text{NaMg}_2\text{V}_3\text{O}_{12}$, *J. Am. Ceram. Soc.* 99 (2015) 399–401.
- [27] H. Zhou, Y. Miao, J. Chen, X. Chen, F. He, D. Ma, Sintering characteristic, crystal structure and microwave dielectric properties of a novel thermally stable ultra-low-firing $\text{Na}_2\text{BiMg}_2\text{V}_3\text{O}_{12}$ ceramic, *J. Mater Sci: Mater Electr.* 25 (2014) 2470–2474.
- [28] F. Liang, X. Fei, S. Congxue, Z. Hui, A Novel Low Firing Microwave Dielectric Ceramic $\text{NaCa}_2\text{Mg}_2\text{V}_3\text{O}_{12}$, *Ceram. Int.* 39 (8) (2013) 9779–9783.
- [29] G.-G. Yao, P. Liu, H.-W. Zhang, Novel Series of Low-Firing Microwave Dielectric Ceramics: $\text{Ca}_5\text{A}_4(\text{VO}_4)_6$ ($\text{A}^{+2} = \text{Mg}, \text{Zn}$), *J. Am. Ceram. Soc.* 96 (6) (2013) 1691–1693.
- [30] R.R. Neurgaonkar, F.A. Hummel, Substitutions in Vanadate Garnets, *Mater. Res. Bull.* 10 (1975) 51–56.
- [31] J.A. Koningstein, O.S. Mortensen, Laser-Excited Phonon Raman Spectrum of Garnets, *J. Mol. Spectrosc.* 27 (1968) 343–350.

- [32] R.K. Moore, W.B. White, T.V. Long, Vibrational spectra of the common silicates. I. Garnets, *Am. Mineral.* 56 (1971) 54-71.
- [33] W.B. White, V.G. Keramidas, Raman Spectra of Yttrium Iron Garnet and two vanadium Garnets, *J. Am. Ceram. Soc.* 54(1971) 472-473.
- [34] H. Liu, L. Yuan, S. Wang, H. Fang, Y. Zhang, C. Hou, S. Feng, Structure, optical spectroscopy properties and thermochromism of $\text{Sm}_3\text{Fe}_5\text{O}_{12}$ garnets, *J. Mater. Chem. C* 4 (2016) 10529-10537.
- [35] Q. Liao, L. Li, X. Ren, X. Ding, New Low-Loss Microwave Dielectric Material ZnTiNbTaO_8 , *J. Am. Ceram. Soc.* 94 (10) (2011) 3237–3240.
- [36] S. Butee, A.R. Kulkarni, O. Prakash, R.P.R.C. Aiyar, I. Wattmwar, D. Bais, K. Sudheeran, R.K.C. James, Significant Enhancement in Quality Factor of Zn_2TiO_4 with Cu-Substitution, *Mater. Sci. Eng. B* 176 (7) (2011) 567–572.
- [37] R.D. Shannon, Dielectric polarizabilities of ions in oxides and fluorides, *J. Appl. Phys.* 73 (1993) 348–366.
- [38] H.Wu, E.S. Kim, Correlations between crystal structure and dielectric properties of high- Q materials in rock-salt structure $\text{Li}_2\text{O-MgO-BO}_2$ ($\text{B} = \text{Ti, Sn, Zr}$) systems at microwave frequency, *RSC Adv.* 6 (2016) 47443-47453.
- [39] H. Zhang, C. Diao, S. Liu, S. Jiang, F. Shi, X. Jing, X-ray diffraction and Raman scattering investigations on $\text{Ba}[\text{Mg}(1-x)/3\text{Zr}_x\text{Ta}_2(1-x)/3]\text{O}_3$ solid solutions, *J. Alloys Compd.* 587 (2014) 717-723.

- [40] C.F. Tseng, Substituting Effects of Zn on Microstructural Characteristics and Microwave Dielectric Properties of $\text{Nd}(\text{Co}_{1/2}\text{Ti}_{1/2})\text{O}_3$ Ceramics, *J. Am. Ceram. Soc.* 91 (12)(2008) 4101–4104.
- [41] B.D. Silverman, Microwave Absorption in Cubic Strontium Titanate, *Phys. Rev.* 125(1962) 1921–1930.
- [42] Z. Fu, P. Liu, J. Ma, X. Zhao, H. Zhang, Novel series of ultra-low loss microwave dielectric ceramics: $\text{Li}_2\text{Mg}_3\text{BO}_6$ ($\text{B} = \text{Ti}, \text{Sn}, \text{Zr}$), *J. Eur. Ceram. Soc.* 36 (3) (2016) 625–629.
- [43] E.S. Kim, B.S. Chun, R. Freer, R.J. Cernik, Effect of packing and bond valence on Microwave dielectric properties of $\text{A}^{2+}\text{B}^{6+}\text{O}_4$ ($\text{A}^{2+} = \text{Ca}, \text{Pb}, \text{Ba}$; $\text{B}^{6+} = \text{Mo}, \text{W}$) ceramics, *J. Eur. Ceram. Soc.* 30 (7) (2010) 1731–1736.